Translational Oncology 22 (2022) 101447

Contents lists available at ScienceDirect

Translational Oncology

journal homepage: www.elsevier.com/locate/tranon

Original Research

TRPC5OS induces tumorigenesis by increasing ENO1-mediated glucose uptake in breast cancer

Yangyang Cui [a,1], Jinghui Peng [a,1], Mingjie Zheng [a,1], Han Ge [a], Xiaowei Wu [a], Yiqin Xia [a], Yue Huang [a], Shui Wang [a], Yongmei Yin [b], Ziyi Fu [b,c,*], Hui Xie [a,*]

[a] Department of Breast Surgery, The First Hospital Affiliated Hospital with Nanjing Medical University, Nanjing 210029, China
[b] Department of Oncology, The First Hospital Affiliated Hospital with Nanjing Medical University, 300 Guangzhou Road, Nanjing 210029, China
[c] Obstetrics and Gynecology Department, Northwestern University, Chicago, IL 60611, USA

ARTICLE INFO

Keywords:
Breast cancer
TRPC5OS
Proliferation
ENO1
Glucose uptake

ABSTRACT

Breast cancer is the most common malignant tumor worldwide and the leading cause of cancer-related deaths in female. Metabolic reprogramming plays critical roles in breast tumorigenesis and induces enhanced glucose uptake and glycolysis. TRPC5OS is encoded by short transient receptor potential channel 5 opposite strand, and predicted to correlate with tumor metabolic reprogramming. Here we aim to elucidate the function of TRPC5OS in aberrant metabolism mediated tumorigenesis. We detected TRPC5OS expression levels in cell lines and tissues by quantitative real-time polymerase chain reaction and immunohistochemistry. Then we assessed the effects of TRPC5OS on proliferation and cell cycle progression in breast cancer cells by cell counting kit-8, colony-formation, EdU-incorporation assays and flow cytometry. Tumor growth *in vivo* was observed in a mouse xenograft model. Mass spectrum analyses were performed to identify potential interactors of TRPC5OS in tumor cells, and the interaction between TRPC5OS and interactors was validated by co-immunoprecipitation (CO-IP), western blots, and immunofluorescent staining. Glucose uptake was measured by liquid scintillation spectrometry. TRPC5OS highly expresses both in breast tumors and cell lines, and might be an independent prognostic marker for breast cancer patients. Overexpressed TRPC5OS promotes breast cancer cell proliferation, cell cycle progression, and enhances tumor xenograft growth. Mass spectral and CO-IP data showed that TRPC5OS interacts with ENO1. We also demonstrate that TRPC5OS could enhance ENO1/PI3K/Akt-mediated glucose uptake in breast cancer cells. Our study demonstrated that TRPC5OS promotes breast tumorigenesis by ENO1/PI3K/Akt-mediated glucose uptake. TRPC5OS might be an independent prognostic marker and potential therapeutic target for breast cancer patients.

Introduction

Breast cancer is one of the most common malignant tumors worldwide and the main cause of cancer-related deaths in women [1]. Globally, there were about 2.1 million newly diagnosed cases of female breast cancer and more than half-a-million related deaths in 2018 [2]. However, our understanding of breast tumorigenesis is still restricted in terms of its prognosis, diagnosis, and therapy, and novel markers, expression signatures, and functional factors are needed to overcome this disease.

Short transient receptor potential channel 5 (TRPC5) has been demonstrated to play a critical role in the development of chemoresistance [3–7]. TRPC5 and p-glycoprotein, the multidrug resistance transporter, were found to be synergistically overexpressed in breast tumor cells after treatment with doxorubicin, resulting in chemoresistance [3]. TRPC5 also played a pivotal role in the extracellular vesicles transport from resistant to wild-type MCF-7 cells, leading to chemoresistance. In circulating extracellular vesicles, the discovery of cancer-specific TRPC5 might thus serve as a prognosis biomarker after chemotherapy [8].

TRPC5 opposite strand (TRPC5OS), also known as *TRPC5* antisense RNA 1 (TRPC5-AS1), is located at chromosome Xq23, and is especially highly expressed in human testis tissue. Cancer-testis (CT) genes are only activated in normal testis and tumors, and their expression

* Corresponding authors.
E-mail addresses: fzyzzu@hotmail.com (Z. Fu), Hxie@njmu.edu.cn (H. Xie).
[1] These authors contribute equally to this study.

https://doi.org/10.1016/j.tranon.2022.101447
Received 25 December 2021; Received in revised form 17 March 2022; Accepted 6 May 2022

characteristics are consistent with the definition of an epigenetic driver gene [9]. Many CT genes have been found to play important regulatory roles in the development of malignant tumors, and breast cancer, especially triple-negative breast cancer, is among the tumors with significant expression of CT genes [10]. In addition, the antisense strands of many important genes may also be involved in cancer progression. For instance, *DSCAM-AS1* was previously reported to mediate tumor progression and tamoxifen resistance by interacting with heterogeneous nuclear ribonucleoprotein L, while *DSCAM* has been shown to be an essential gene controlling cell-intrinsic aspects of dendrite guidance in all four classes of dendrite arborization neurons [11,12]. Furthermore, upregulation of *HOXA10-AS* induced by ETS-like protein 1 promoted lung adenocarcinoma progression by increasing Wnt/β-catenin signaling, and *HOXA10* could direct the ability of proliferation and invasion in gastric cancer cells [13,14]. In view of its antisense strand, TRPC5 was important in breast cancer chemoresistance, and may also be associated with the progression of breast cancer. However, the function of TRPC5OS in the progression of diseases is poorly understood.

Interestingly, *TRPC5OS* was translated as a microprotein of 111 amino acids. Microproteins are proteins of about 100 amino acids, which have demonstrated important roles in biology and disease [15–18]. Microproteins are produced through ribosomal translation of small open reading frames, and transcripts, annotated as long non-coding RNAs, may also encode microproteins [19–21]. Microproteins function by disturbing the formation of higher order protein complexes at the molecular level [22]. Several microproteins have been shown to have strong effects on biological processes in plants and animals. In human cells, HUMANIN and MOTS-C were identified as regulating factors in mitochondrial physiology, while the mRNA-decapping complex was shown to be made of NOBODY, and MRI-2 stimulated the non-homologous end joining of DNA [16,23,24,25]. Microproteins, which function as dominant regulators in a targeted way, have great potential for biotechnological applications.

Here, we investigated the expression pattern of TRPC5OS in breast tumors and its potential roles in breast tumorigenesis, which might afford potential prognostic marker and novel therapeutic target for breast cancer patients.

Materials and methods

Cell lines and cell culture

The human cancer cell lines A549, HCC-827, NCI-H1299, Beas-2B, GES-1, and HGC-27were provided by Professor Yongqian Shu (Nanjing Medical University, Nanjing, China), FHC, DLD-1, HCT116, and LoVo cells were gifted by Yueming Sun (Nanjing Medical University, Nanjing, China), JIMT-1 cells were obtained from Professor Yongmei Yin (Nanjing Medical University, Nanjing, China), MCF-10A, MDA-MB-231, ZR-75–1, BT474, MDA-MB-453, SK-BR-3, HCC1937, and MCF-7 cells were from Ziyi Fu (Northwestern University, Chicago, IL, USA), and SUM-1315 cells were gifted by Stephen Ethier (University of Michigan, Ann Arbor, MI, USA). All cells were incubated in high-glucose Dulbecco's modified Eagle medium which contained 100 U/mL penicillin, 100 mg/mL streptomycin, and 10% fetal bovine serum (Gibco, Australia) in a humidification incubator with 95% air and 5% CO_2 at 37°C.

Patient tissue samples

Approval for this research was obtained from the Ethics Committees of Jiangsu Province Hospital (the First Hospital Affiliated Hospital with Nanjing Medical University). Mammary tumor and adjacent normal tissues were acquired from Jiangsu Province Hospital, after obtaining informed consent from each patient (Patients' information is in Supplementary File 1). All samples were from mammary tumor patients who had not undergone any endocrine therapy or chemotherapy prior to operative treatment. All excised samples were preserved immediately in −80 °C refrigerator.

Tissue microarray (TMA) and immunohistochemistry

Separate TMAs (12×8) were constructed from 96 mammary tumor and corresponding adjacent normal tissues, respectively, and kept at 4 °C until analysis. Before decreasing concentrations of ethanol, the TMAs were treated using xylene and 100% ethanol. The antigen retrieval: put the sample slide holder in the citrate buffer above 95 ℃, incubate in a water bath above 95 ℃ for more than 20 min, take out the incubator and place it at room temperature for at least 20 min. Step 2: put the incubator in the microwave oven, heat it to boiling, stop immediately, rinse the outer surface of the incubator with tap water, cool, put the incubator into the microwave oven again after cooling, heat it to boiling, stop immediately, rinse the outer surface of the incubator with tap water, cool, repeat three times. After antigen retrieval, the TMAs were blocked and then incubated with anti-TRPC5OS (Quan-biotech, Wuhan, China), followed by incubation with secondary antibody using the typical avidin-biotin-peroxidase complex method. Samples were counterstained with hematoxylin and images were obtained using an upright light microscope (Nikon, Japan). The method for the scoring of signal intensity on IHC slides was H-SCORE=∑(PI×I)=(percentage of cells of weak intensity ×1)+(percentage of cells of moderate intensity ×2)+percentage of cells of strong intensity ×3).

Lentivirus transfection

TRPC5OS overexpression/knockdown lentiviruses and negative controls (NC, LV5/LV3) were all obtained from GenePharma (Shanghai, China). MCF-7, MDA-MB-231, and SUM1315 cells were transfected with LV-TRPC5OS and LV-NC (LV5) at 40%–50% confluence for TRPC5OS overexpression, or with sh-TRPC5OS (193) and sh-Ctrl (LV3) for TRPC5OS repression. Finally, we selected breast cancer cells populations that is steady and agminated using puromycin (VWR, City, PA, USA) at the concentration of 4 μg/mL for 2 weeks.

Plasmid and small interfering RNA (siRNA) transfection

Cells were transfected with ENO1 plasmids (pEX-3: an empty vector used as a control) and siRNAs (NC: non-targeting sequence used as a control,GenePharma, Shanghai, China) for overexpression and repression, respectively, using Lipofectamine 3000 (Invitrogen, Carlsbad, CA, USA), on the basis of the protocols of manufacturer.

Cell counting kit-8 (CCK-8) assay

2×10^3 cells/well breast cancer cells were incubated onto 96-well plates overnight, followed by further incubation for 1, 2, 3, 4, 5, or 6 days at 37 °C and 5% CO_2. CCK8 labeling reagent (10 μL, 0.5 mg/mL; Dojindo, Japan) was then mixed in each well, and incubation was continued for 2 h at 37 °C and 5% CO_2. The cells were analyzed by measuring their absorption at 450 nm using an enzyme-labeled meter (Thermo Scientific, Shanghai, China).

Colony-formation assay in vitro

500 cells/well breast cancer cells were incubated onto 6-well plates for 2 weeks. The cells were then washed using phosphate-buffered saline (PBS) for three times and cell staining was performed using crystal violet (Beyotime, Shanghai, China). The number of colonies in each well was counted.

5-Ethynyl-2′-deoxyuridine (EdU) assay

Cells were seeded onto 24-well plates at a density of 1×10^4 cells/

well and incubated overnight. Cells were stained with an EdU kit (RiboBio, Guangzhou, China), and photographed by fluorescence microscopy (Nikon).

Cell cycle analysis by flow cytometry

Cells were collected, washed and fixed under the condition of −20 °C for one day. The cells were washed again, stained using propidium iodide, and treated with a cell cycle analysis kit (MultiSciences, Hangzhou, China) according to the manufacturer's instructions. The cell cycle characteristics were then analyzed using a FACScan flow cytometer (BD Bioscience, Franklin Lakes, NJ, USA). The gray is the G1 phase, the purple is the S phase, the blue is the G2 phase.

RNA extraction and quality control

Total RNA was extracted from tissues and cells using RNAiso plus (Takara, Japan) according to the manufacturer's protocol, and dissolved in RNase-free water. The quality and concentration of the RNA were measured using a NanoDrop ND-1000 spectrophotometer (NanoDrop Technologies, Wilmington, DE, USA). Finally, all the samples were frozen at –80 °C.

qRT-PCR

The RNA was reverse transcribed to cDNA using a reverse transcription kit (Takara) followed by qRT-PCR using a SYBR Green Master Mix Kit (Roche, Reinach, Switzerland) with a LightCycler 480® Real Time PCR System (Roche). The level of the target mRNA expression was normalized to that of glyceraldehyde 3-phosphgate dehydrogenase. Finally, the relative expression levels were aquired according to the ΔΔCT and $2^{-\Delta\Delta Ct}$ method. Each PCR amplification was conducted at least for three times.

Primers for ENO1 are forward primer: 5′-AAGCTGGTGCCGTTGAGAA-3′, reverse primer:5′-GGTTGTGGTAAACCTCTGCTC-3′, TRPC5OS: forward primer: 5′-ACTGCAGGACCATAGTTGGA-3′, reverse primer: 5′-CCACCGGTCTCCACCTTAAA-3′, and GAPDH: forward primer: 5′-GCTGCGAAGTGGAAACCTAC-3′, reverse primer: 5′-CCTCCTTCTGCA CACATTTGAA-3′.

Western blot analysis

Western blot analysis was conducted as introduced previously [26], using the following antibodies: anti-TRPC5OS (Quan-biotech, Wuhan, China), anti-ENO1 (Abcam, Cambridge, MA, USA), anti-PI3K (Abcam), anti-pPI3K (Abcam), anti-Akt (Abcam), anti-phospho-Akt (Abcam), and anti-β-actin (Cell Signaling, Danvers, MA, USA). β-Actin was used as an internal control. Peroxidase-conjugated Affinipure goat anti-mouse and anti-rabbit IgG (H+L,Jackson Immunoresearch, City, PA, USA) were utilized as secondary antibodies.

Co-immunoprecipitation

Protein was extracted from 1×10^7 cells and immunoprecipitated using anti-ENO1 and anti-TRPC5OS, with rabbit IgG as a control, according to the manufacturer's instructions of Thermo Pierce Co-Immunoprecipitation Kit (Thermo Scientific, Scotts Valley, CA, USA), followed by immunoblotting and mass spectrometry analysis.

Immunofluorescent staining

MCF-7 and MDA-MB-231 cells were plated and cultured on glass coverslips for 72 h, fixed in 4% formalin for 20 min, permeabilized in 0.1% Triton X-100, and then blocked with 4% bovine serum albumin. The cells were then incubated with primary antibodies overnight at 4 °C followed by fluorescein isothiocyanate- or Cy3-conjugated antibodies (Jackson Immunoresearch). The cells were co-stained with DAPI to detect the nuclei, followed by fluorescence analysis under a fluorescence microscope (Nikon, Tokyo, Japan).

Measurement of glucose uptake

3×10^5 cells/well breast cancer cells were incubated onto 6-well plates overnight. The cells were then washed with PBS and cultivated in 3 mL of Krebs–Ringer–HEPES (KRH) buffer (25 mM HEPES, pH 7.4, 120 mM NaCl, 5 mM KCl, 1.2 mM $MgSO_4$, 1.3 mM $CaCl_2$, and 1.3 mM KH_2PO_4) containing 1 μCi of [^{3}H]−2-deoxyglucose (PerkinElmer Life Sciences, USA) for 30 min, followed by washing in ice-cold KRH buffer to stop the uptake, and dissolving in 300 μL of lysis buffer (10 mM Tris–HCl, pH 8.0, 0.2% sodium dodecyl sulfate). The level of radioactivity per aliquot was detected using a liquid scintillation spectrometer and the intracellular level of [^{3}H]−2-deoxyglucose was calculated based on the number of disintegrations per minute.

Subcutaneous xenograft models in vivo

The animal studies were approved by the Institutional Animal Care and Use Committee, Nanjing Medical University (approval number IAUCU-1,708,006). Balb/c nude mice (female, 3–4 weeks old) were bought from the Model Animal Research Center, Nanjing University, and raised in the university's Animal Core Facility under specific pathogen-free conditions. Twenty mice were allocated randomly into four groups and SUM-1315/TRPC5OS, SUM-1315/LV5, SUM-1315/193, and SUM-1315/LV3 cells respectively (2×10^6 cells in 0.1 mL PBS per mouse) were injected into the left side of the second pair of mammary gland fat pads subcutaneously under inhalation anesthesia with 3% isoflurane. Weight loss was determined every week. Tumor volume was monitored per week and evaluated by formula: total tumor volume (mm^3) = length×width^2/2. Mice were executed by cervical dislocation if the size of solid tumors is more than 10 percent of the animal's body weight. After 10 min, if the animal's vital signs, such as respiration, heartbeat, corneal reflexes, muscle tone, and mucous membrane color disappeared, the death was determined. All the 20 mice were euthanized and no premature death occurred. Tumor specimens were resected on day 28, measured, and weighed, followed by fixation in 10% buffered formalin. The mice were sacrificed by cervical dislocation after 4 weeks.

Mass spectrometry analysis and data analysis

In LC-MS/MS, the chromatographic separation of samples was performed on a Poroshell 120 C18 column (2.7 μm, 2.1 mm×30 mm; Agilent Technologies, USA) at room temperature. The mobile phase consists of phase A (0.1% formic acid/pure water) and phase B (100% acetonitrile). The flow rate of the mobile phase is 0.3 mL/min, and the concentration gradient is B 10% (0 min) → 10% (1 min) → 90% (4 min) → 90% (8 min) → 10% (9 min). Each injection is 5 μL. The mass spectrometer is connected to the ion source (ESI), and the positive ion mode of MRM is selected. Both Q1 and Q3 are set at the unit resolution (Unit). The flow rate of the drying gas is 10 L/min, and its temperature is maintained at 350 °C. The best electrocapillary voltage is 5500 V. The atomizer pressure is set to 35 psi. The data is collected and processed by AB SCIEX workstation software (Analyst Software lnk). Peptides are monitored in multiple reaction monitoring mode (MRM).

Data analysis and TMT quantification

Proteome discoverer software (version 1.4,Thermo Scientific, USA) was used to perform database searching against the RefSeq human protein sequence database from the NCBI using the Sequest algorithms. The search parameters are specified as follows: The mass tolerance of precursor ions was set to 15 ppm, and the mass tolerance of fragment

ions was set to 20mmU. Trypsin was designated as a digestive enzyme and we allowed 2 missed cleavages. Cysteine aminomethylation and TMT modification (N-terminal and lysine residues) were defined as fixed modifications, and methionine oxidation was defined as variable modification. The false positive detection rate (FDR) was calculated by searching the bait database. Filter the results using the following settings: only high confidence peptides based on the global FDR of the target bait method < 1% were included. In the TMT quantitative

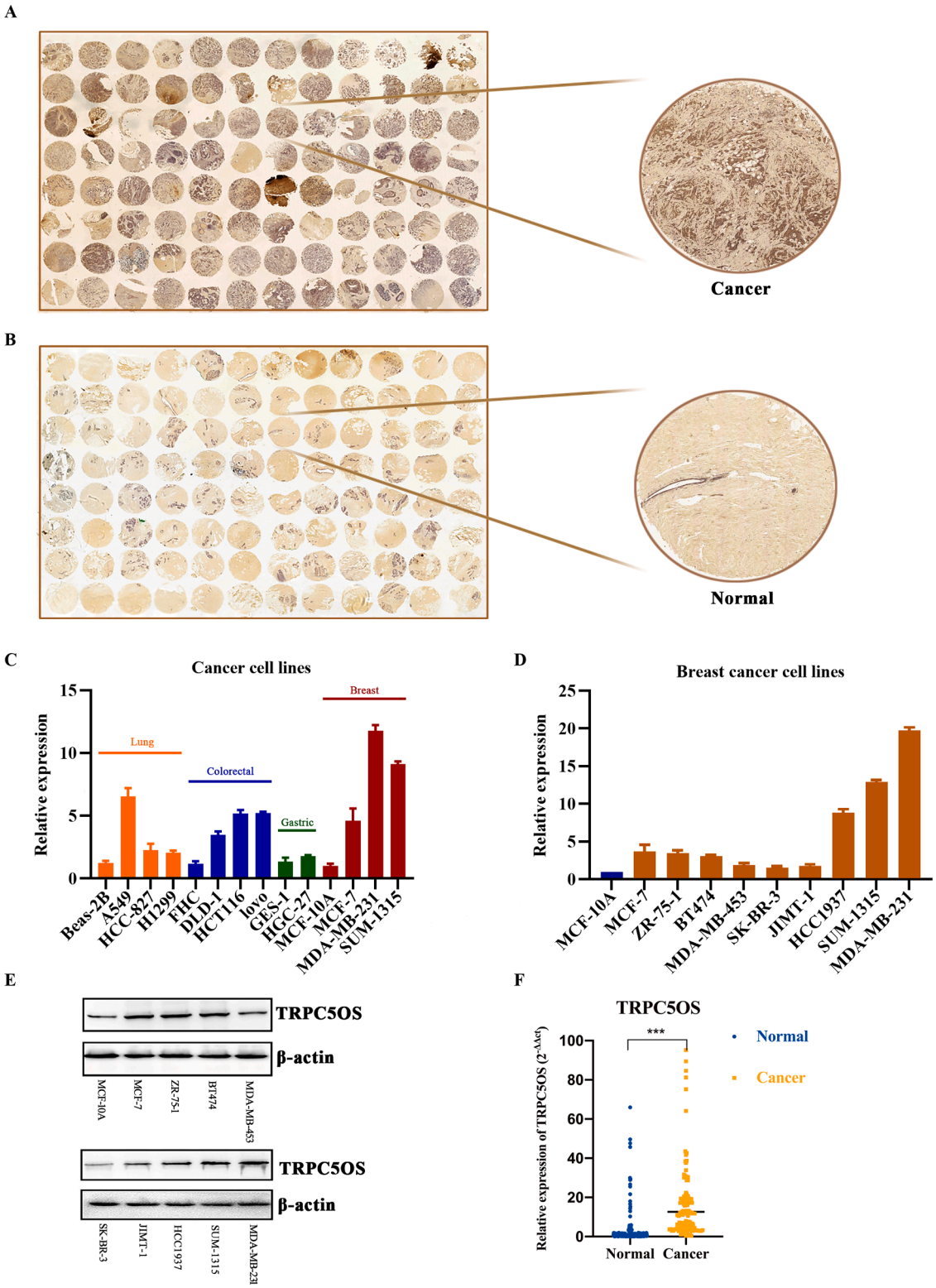

Fig. 1. Identification and characterization of TRPC5OS overexpression in breast cancer.
Expression of TRPC5OS in 96 paired human breast cancer and adjacent normal tissue TMAs was determined by immunohistochemistry (A, B). Expression of TRPC5OS mRNA in cancer cell lines was detected by qRT-PCR (C). TRPC5OS mRNA and protein expression levels in breast cancer cell lines and MCF-10A cells detected by qRT-PCR and western blot, respectively (D, E). TRPC5OS expression in breast cancer tissues and normal tissues (F).

workflow, the most reliable centroid method was used, and the integral window was 20 ppm. For protein quantification, only unique peptides were used to quantify proteins.

Statistical analysis

Statistical analysis was conducted using SPSS version 20.0 (SPSS, Chicago, IL, USA) and GraphPad Prism 6 (GraphPad Software, CA, USA). Differences between two clinical groups were analyzed by paired *t*-tests. Correlations between TRPC5OS and clinical pathological parameters were analyzed by χ^2 tests. Statistical significance was set at $P<0.05$. All results were based on an average of at least three independent experiments.

Results

TRPC5OS overexpressed both in breast cancer tissues and cell lines

We examined TRPC5OS expression by immunohistochemistry in two TMAs including 96 paired samples, to compare its expression profiles between normal and breast cancer samples. adjacent normal tissues TRPC5OS expression was higher than that of adjacent normal tissues in breast cancer (Fig. 1A,B). We also verified TRPC5OS mRNA expression levels in human lung, colorectal, gastric, and breast cancer cells by qRT-PCR. TRPC5OS mRNA expression levels were increased to different degrees in cancer cell lines, especially breast cancer cells (Fig. 1C).

Further, TRPC5OS mRNA and protein levels in MCF-10A and breast cancer cell lines (MCF-7, ZR-75–1, MDA-MB-453, SK-BR-3, JIMT-1, BT474, HCC1937, MDA-MB-231, SUM1315) were determined by qRT-PCR and western blot, respectively. TRPC5OS expression was higher in all breast cancer cell lines, especially MCF-7, ZR-75–1, HCC1937, MDA-MB-231, and SUM1315 cells (Fig. 1D,E). We validated the TRPC5OS mRNA expression levels in 150 breast cancer tissue samples and normal tissue samples using mRNA qRT-PCR. The result showed that TRPC5OS was overexpressed in breast cancer tissue samples (Fig. 1F). These results, together with the results in cell lines, indicated that TRPC5OS expression was enhanced in breast cancer cells, suggesting a potential tumorigenic function.

TRPC5OS promotes breast cancer cell proliferation in vitro

TRPC5OS or shTRPC5OS (193) lentivirus constructs were transfected into MCF-7, MDA-MB-231, and SUM-1315 cells, and TRPC5OS mRNA and protein levels were detected by qRT-PCR and western blot, respectively (Fig. 2A,B). The biological functions of TRPC5OS in breast cancer cell lines were then investigated.

The effects of TRPC5OS overexpression on the viability of MCF-7, MDA-MB-231, and SUM-1315 cells was determined by CCK8 assay. Cell viabilities were significantly increased by TRPC5OS overexpression, compared with control cells transfected with NC (LV5) vectors (Fig. 2C). We also assessed colony formation in the same breast cancer lines, and showed that compared with LV5, TRPC5OS overexpression significantly increased the number and area of colonies (Fig. 2E). Furthermore, the percentage of EdU-positive cells was increased by TRPC5OS overexpression (Fig. 2G-J).

We further validated the effect of TRPC5OS on breast cancer cell viability by carrying out CCK8, colony-formation assays and EdU-incorporation assays in cells transfected with shTRPC5OS (193). Knockdown of TRPC5OS in breast cancer cells inhibited cell growth, suppressed colony formation, and reduced the percentage of EdU-positive cells (Fig. 2D, F, G-J).

Overall, we found that TRPC5OS may promote the viability and proliferation of breast cancer cell lines. In addition, TRPC5OS overexpression could also favor cell cycle progression of breast cancer cells from S phase to G2 phase, further supporting the involvement of TRPC5OS in the growth of breast cancer cells (Fig. 3A,B).

TRPC5OS promotes tumor growth in vivo

We assessed the role of TRPC5OS on tumor growth *in vivo* by subcutaneously implanting SUM-1315/TRPC5OS, SUM-1315/LV5, SUM-1315/193, and SUM-1315/LV3 cells into nude mice. The volumes and weights of the tumors were recorded 4 weeks after inoculated. The volumes and weights of SUM1315 tumors overexpressing TRPC5OS were larger than tumors in the control group, while tumors in the knockdown group were obviously smaller than those in the control group (Fig. 3C,D). In line with the cell proliferation results *in vitro*, TRPC5OS significantly increased tumor volume *in vivo*, thus confirming its involvement in the growth of breast cancer cells (Fig. 3E,F). The expression of TRPC5OS in the tumors and the growth curve of the tumors are provided in Fig. S3.

TRPC5OS interacts with ENO1 and regulates its protein levels

The small size of microproteins means that most microproteins lack the multifunction domain structure of classical proteins, and are thus usually thought to play their roles via complexation with proteins or in large protein assemblies [27–29]. We investigated TRPC5OS-associated proteins by immunoprecipitation with anti-TRPC5OS followed by mass spectrometry analysis. Filtering of the proteomics data identified all the TRPC5OS-interacting proteins, which were particularly enriched in the TRPC5OS compared with IgG immunoprecipitation group in triplicate experiments. Following this stringent analysis, 11 unique proteins were selected, including annexin A1 (ANXA1), peroxiredoxin-1 (PRDX1), elongation factor 1-delta (EEF1D), eukaryotic translation elongation factor 1 gamma (EEF1G), ENO1, lactate dehydrogenase b (LDHB), filamin-C (FLNC), ribosomal protein S3 (RPS3), heterogeneous nuclear ribonucleoprotein D (HNRNPND), lipocalin-1(LCN1) and protein S100-A7 (Fig. 4A). Importantly, ENO1 and LDHB are both key enzymes in glycolysis, and ENO1 has been shown to promote cell proliferation by modulating the PI3K/Akt signaling pathway and to induce tumorigenesis by activating plasminogen [30]. We therefore chose to investigate ENO1 further.

We validated the interaction between ENO1 and TRPC5OS by immunoprecipitation, and subjected the pulled-down lysates to western blot analysis. In accordance with the proteomics data, ENO1 protein was abundant in the anti-TRPC5OS but not in the IgG sample (Fig. 4B). In addition, immunofluorescent staining showed that TRPC5OS co-localized with ENO1 in both the cytoplasm and nucleus (Fig. 4C).

ENO1 is also an oncogene, and its overexpression has been related to many kinds of tumors, including cholangiocarcinoma, thyroid carcinoma, lung cancer, hepatocellular carcinoma, glioma, neuroendocrine tumors, neuroblastoma, pancreatic cancer, prostate cancer, and gastric cancer [30–38]. We therefore analyzed ENO1 mRNA expression in 100 pairs of breast cancer samples to demonstrate its association with breast cancer. Compared with the normal breast tissues, ENO1 mRNA was significantly up-regulated in the tumor samples (Fig. 4E). It indicated that there is a positive correlation between the expression level of TRPC5OS mRNA and that of ENO1 mRNA. We also investigated the correlation between TRPC5OS protein expression and ENO1 protein levels by quantifying ENO1 levels after stable overexpression of TRPC5OS in MCF-7, MDA-MB-231, and SUM-1315 cells. TRPC5OS overexpression increased ENO1 protein levels (Fig. 4F), but ENO1 mRNA levels remained unchanged (Fig. 4D), suggesting that TRPC5OS may affect the posttranscriptional or posttranslational modification of ENO1. In turn, ENO1 protein levels were significantly reduced by TRPC5OS knockdown in MCF-7, MDA-MB-231, and SUM-1315 cells, while mRNA levels were again unchanged (Fig. 4D,F).

TRPC5OS actives the PI3K/Akt pathway and regulates glucose uptake in breast cancer cell lines

ENO1 has previously been linked to regulation of the proliferation

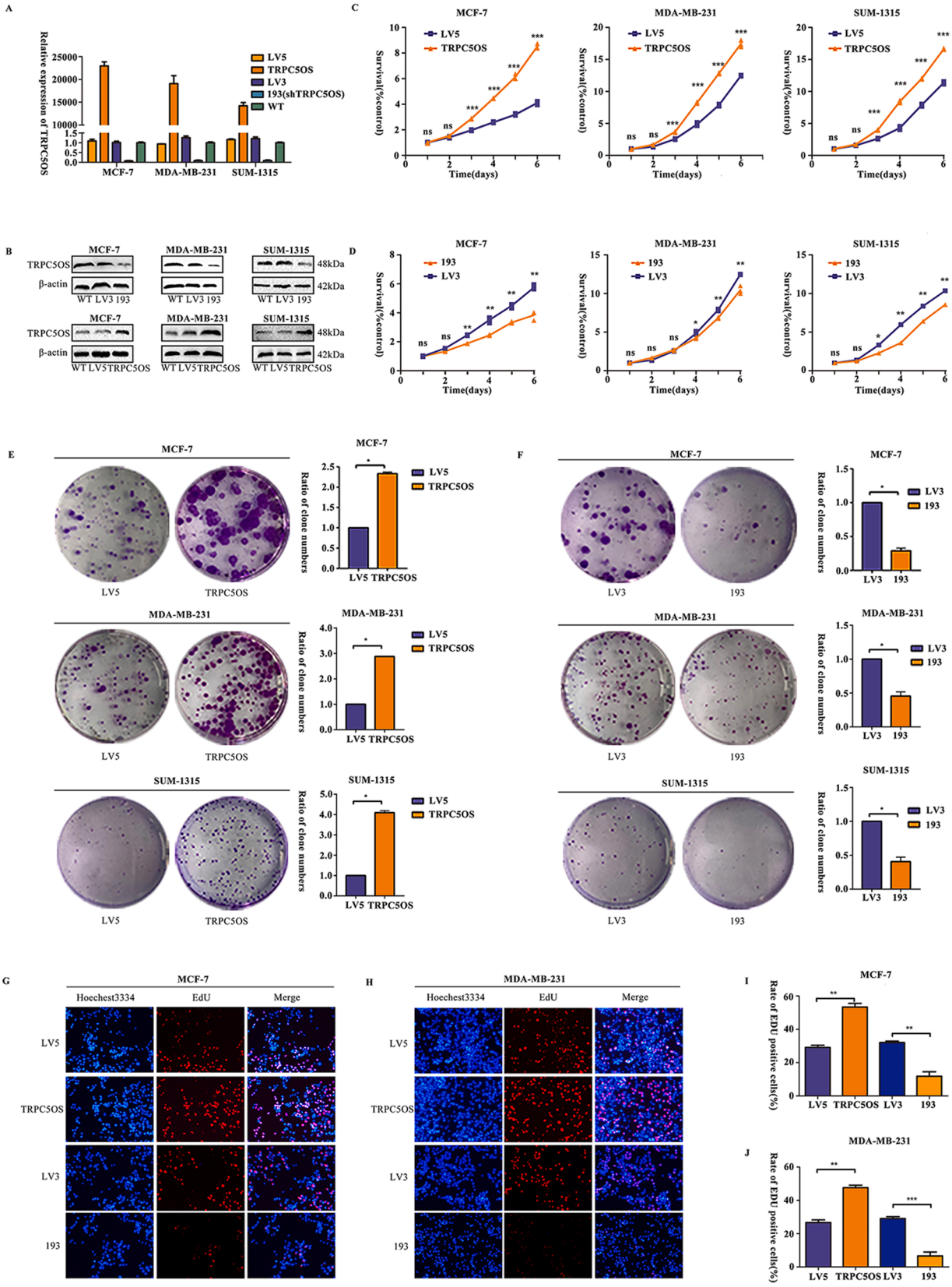

Fig. 2. TRPC5OS promotes breast cancer cell proliferation *in vitro*.
TRPC5OS mRNA and protein expression levels in breast cancer cells transfected with TRPC5OS or shTRPC5OS (193) lentivirus were detected by qRT-PCR and western blot, respectively (A, B). Proliferation of TRPC5OS-overexpressing or -repressed cells was determined by CCK-8, colony-formation, and EdU-incorporation assays (C-J).

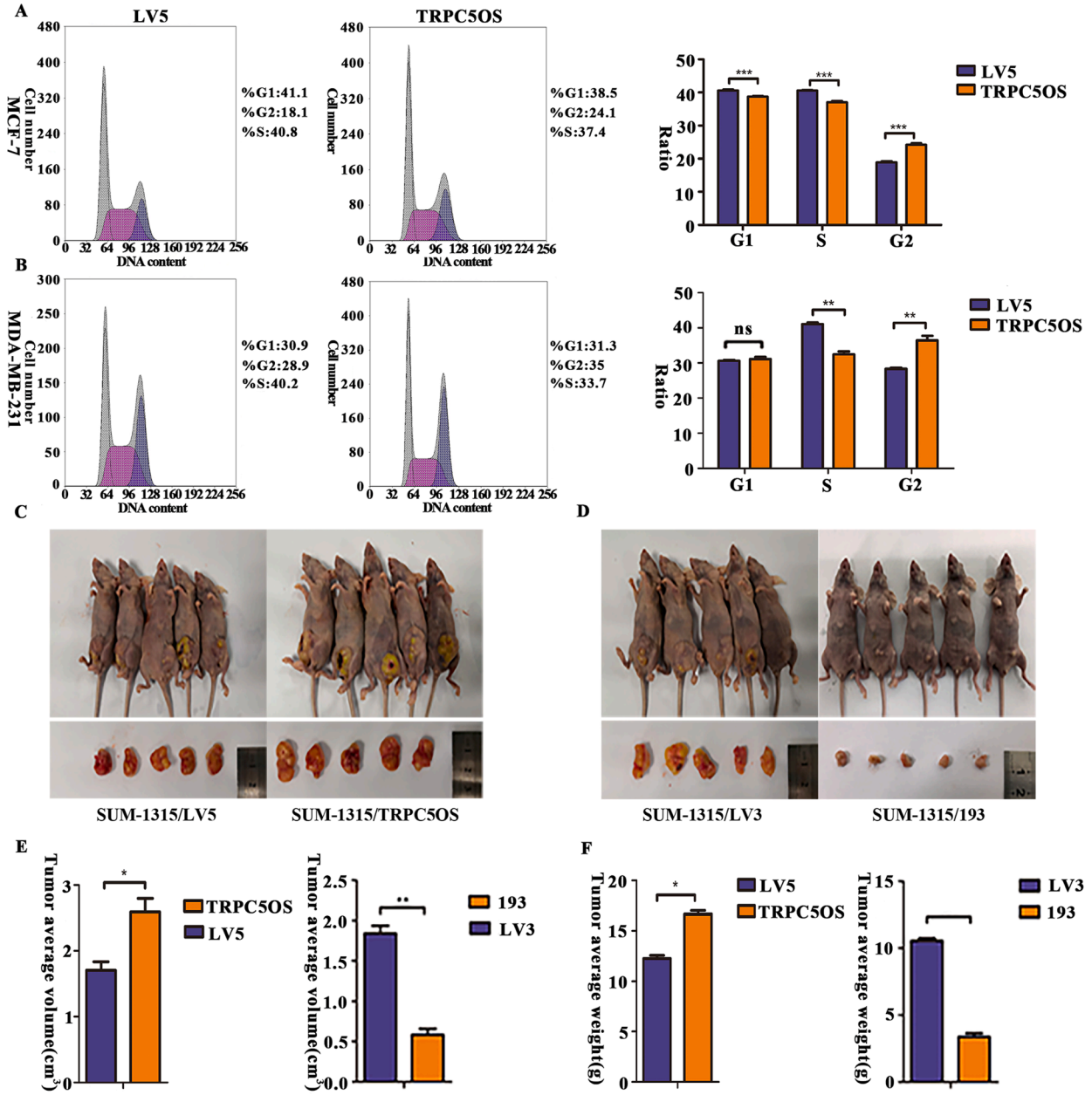

Fig. 3. TRPC5OS promotes cell cycle progression and tumor growth in a nude mouse model of SUM-1315 cells *in vivo*.
The cell cycle of TRPC5OS-overexpressing and control cells was analyzed by flow cytometry (A, B). Subcutaneous tumors formed in nude mice following injection of TRPC5OS-overexpressing or -repressed SUM-1315 cells, compared with controls (C, D). Tumor growth and weight (E, F). Average tumor volume and weight are expressed as the mean ± standard deviation for five mice. **P*<0.05; ***P*<0.01; ****P*<0.001.

ability of cells by affecting PI3K and Akt phosphorylation [31]. We therefore determined if TRPC5OS overexpression affected the activity of the PI3K/Akt pathway through conjugation with ENO1. Overexpression of TRPC5OS significantly increased levels of total and phosphorylated PI3K and Akt, as determined by specific antibodies (Fig. 5A,C), while TRPC5OS knockdown reduced levels of the total and phosphorylated proteins (Fig. 5B,D).

ENO1 plays an essential role in the glycolysis process, and participates in glucose metabolism by promoting glycolysis [30]. We therefore investigated the effect of TRPC5OS on the regulation of glucose uptake. Overexpression of TRPC5OS increased glucose uptake in MCF-7 and SUM-1315 cells, while knockdown of TRPC5OS reduced glucose uptake (Fig. 5E).

These results indicated that TRPC5OS may be involved in the PI3K/Akt pathway and in glycolysis regulated by ENO1.

ENO1 is the functional target of TRPC5OS in breast cancer cells

We confirmed the role of ENO1 in mediating the effects of TRPC5OS in breast cancer by transfecting MCF-7, MDA-MB-231, and SUM-1315 cells with ENO1-overexpression plasmids or siRNAs, respectively (Fig. S1A–C). ENO1 overexpression promoted cell proliferation, consistent with the effects of TRPC5OS overexpression (Fig. 5F, H). In contrast, down-regulation of ENO1 inhibited cell proliferation, also in accordance with the effects of TRPC5OS down-regulation (Fig. 5G, I).

In addition, we investigated the ability of ENO1 to neutralize the effects of TRPC5OS overexpression. ENO1 expression was abrogated by transfection with ENO1 siRNAs or enhanced by transfection with ENO1 plasmids (Fig. 6A,C). TRPC5OS-induced proliferation and increasing glucose uptake was effectively reversed by silencing ENO1 (Fig. 6B, E-H; Fig S2A, B). Similarly, ENO1 overexpression in cells transfected with sh-

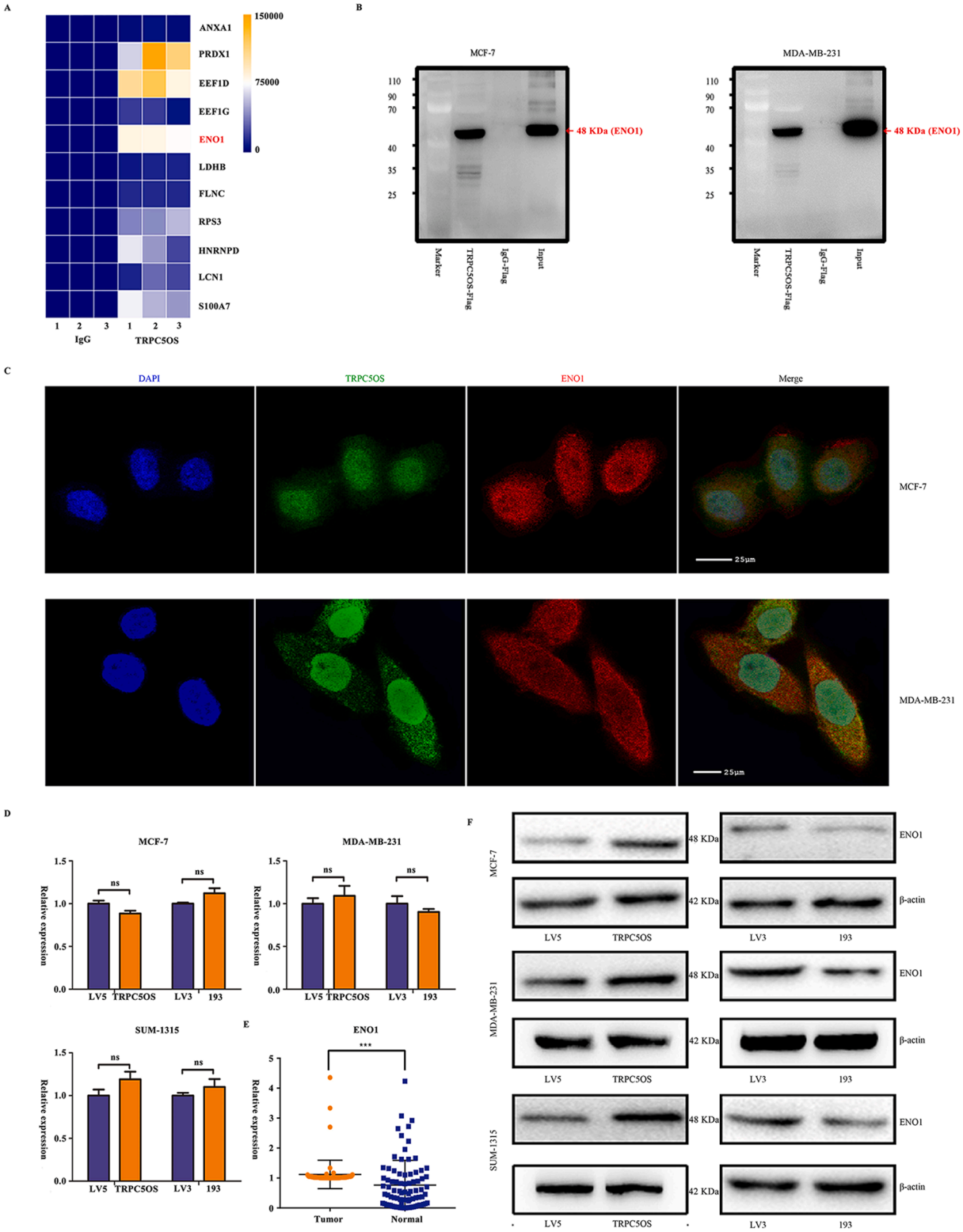

Fig. 4. TRPC5OS interacts with alpha-enolase (ENO1) and regulates ENO1 protein levels.
TRPC5OS-interacting proteins were identified by filtering the proteomics data (A). The interaction between ENO1 and TRPC5OS was validated by immunoprecipitation and western blot analysis (B). TRPC5OS co-localized with ENO1 in both the cytoplasm and nucleus, as shown by immunofluorescent staining (C). ENO1 mRNA expression in 100 paired human breast cancer and adjacent normal tissues was determined by qRT-PCR (E). ENO1 mRNA and protein expression in TRPC5OS-overexpressing and -repressed cells investigated by qRT-PCR and western blot analysis, respectively (D, F).

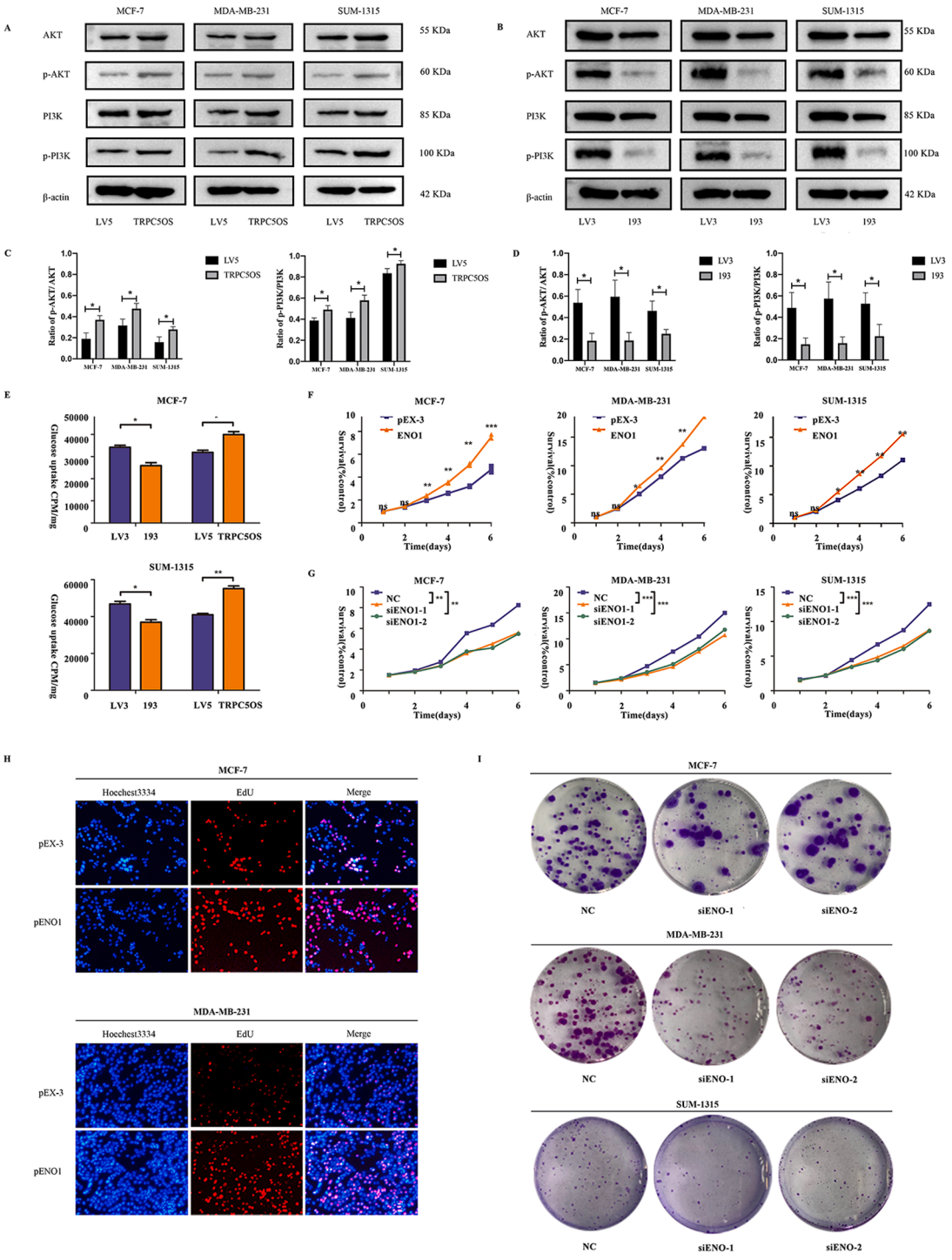

Fig. 5. TRPC5OS activates the PI3K/Akt pathway and regulates glucose uptake in breast cancer cell lines.
Levels of total and phosphorylated PI3K and Akt in TRPC5OS-overexpressing and -repressed breast cancer cells were detected by western blot analysis (A, B). Bar graphs of the ratio of phosphoPI3K/total PI3K, phosphoAkt/total Akt in TRPC5OS-overexpressing or -repressed breast cancer cells (C, D). Glucose uptake in TRPC5OS-overexpressing and -repressed cells was investigated by liquid scintillation spectrometry (E). Viability of ENO1-overexpressing and -repressed breast cancer cells was determined by CCK8 assay, colony-formation, and EdU-incorporation assays (F-I).

TRPC5OS (193) lentivirus neutralized the consequences of TRPC5OS knockdown (Fig. 6D, I-L; Fig. S2C,D).

Overall, these results suggest that ENO1 can serve as the target of TRPC5OS in breast cancer cells.

TRPC5OS expression is a potential prognostic index for human breast cancer

Based on the above studies, we further investigated the clinical significance of TRPC5OS expression in human breast carcinoma. Regarding tumor size, patients expressing high levels of TRPC5OS had larger tumors than patients expressing low levels of TRPC5OS (Fig. 7A).

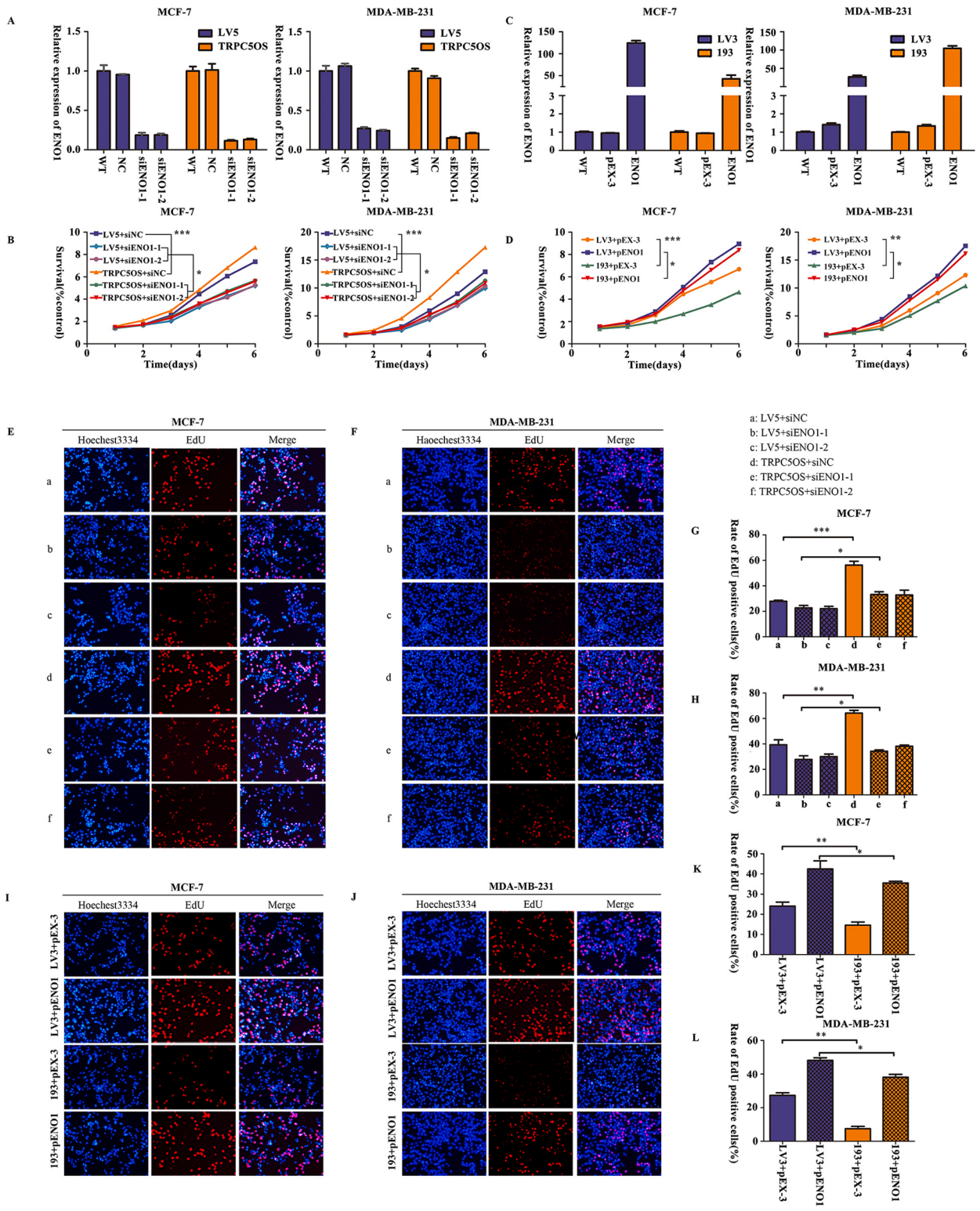

Fig. 6. ENO1 is the functional target of TRPC5OS in breast cancer cells.
ENO1 expression in TRPC5OS-overexpressing breast cancer cells transfected with ENO1 siRNAs was detected by qRT-PCR (A). ENO1 expression in TRPC5OS-repressed breast cancer cells transfected with ENO1 plasmids was detected by qRT-PCR (C). Proliferation of TRPC5OS-overexpressing/ENO1-repressed and TRPC5OS-repressed/ENO1-overexpressing breast cancer cells were analyzed by CCK-8 and EdU-incorporation assays (B, D-L).

Similarly, TRPC5OS expression levels were strongly related to tumor grade (Fig. 7B). We also examined the correlation between clinical molecular subtypes (estrogen receptor [ER], progesterone receptor [PR], HER-2, Ki-67) and TRPC5OS levels, given that the prognosis and treatment of breast cancer differ according to these molecular subtypes. A total of 40/50 breast cancer patients expressing high TRPC5OS were HER-2 negative, and 30/50 of breast cancer patients expressing low TRPC5OS were HER-2 positive (Fig. 7D). A total of 27/50 breast cancer patients expressing high levels of TRPC5OS showed high Ki-67 levels, compared with only 15/50 patients with low TRPC5OS expression

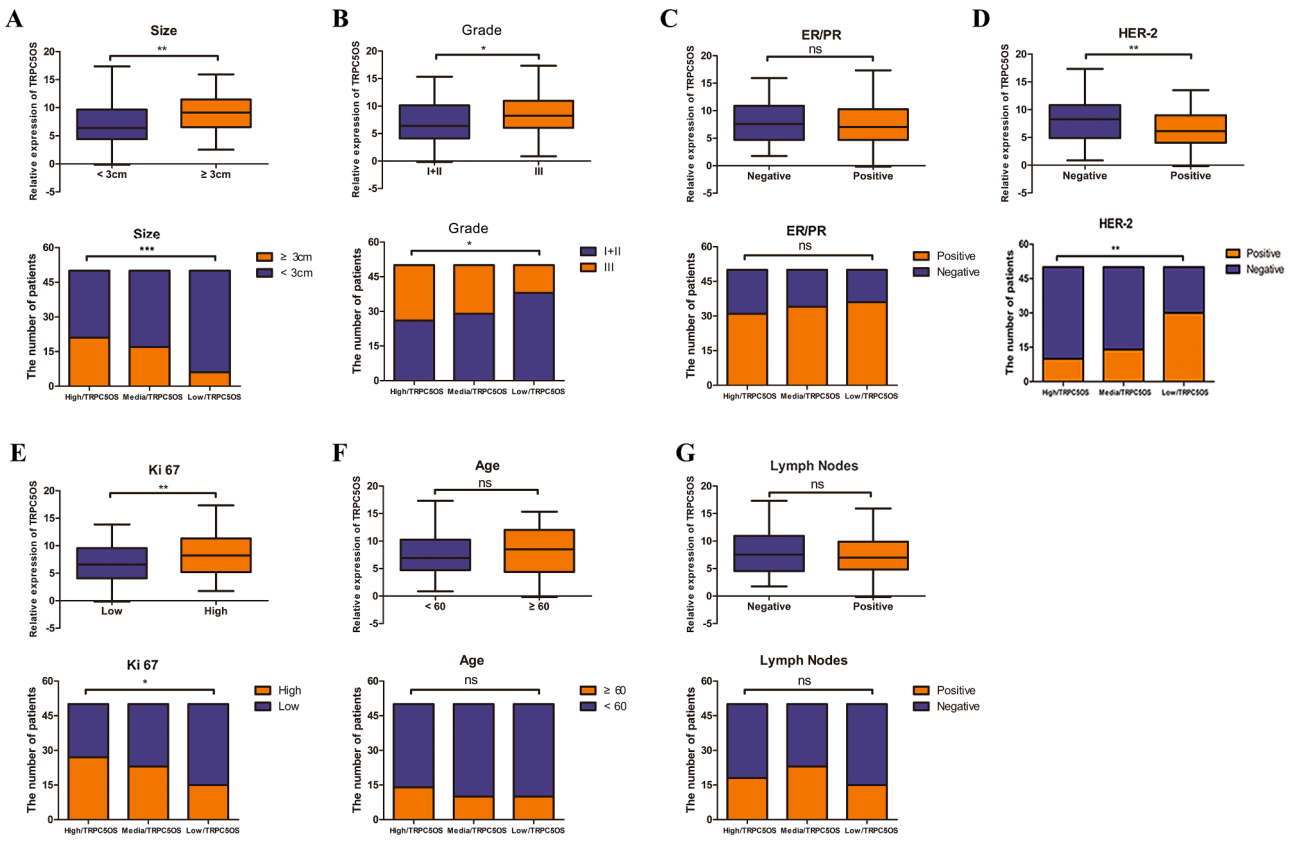

Fig. 7. TRPC5OS expression is a potential prognostic index for human breast cancer.
Correlations between TRPC5OS expression levels in breast cancer tissues and clinical parameters: tumor size, tumor grade, ER/PR, HER-2, Ki-67, age, and positive lymph nodes (A-G).

(Fig. 7E). However, there were no significant differences in ER and PR expression, patient age, and axillary lymph node positivity between the high-expression and low-expression TRPC5OS groups among the 150 samples studied (Fig. 7C,F,G). These clinical data suggest that TRPC5OS was a potential prognostic index in breast cancer patients.

Discussion

Tumor is often thought to be induced by gene expression disorder in cells. Identifying and analyzing the functions of key participants may thus improve our understanding of the processes linked to cancer transformation. In this study, we identified and characterized a new gene, TRPC5OS. TRPC5OS expression was enhanced in breast cancer samples and overexpression of TRPC5OS increased proliferation of breast cancer cells, promoted progression of cell cycle, and enhanced growth of xenograft tumor, associated with the PI3K-Akt pathway.

In the current research, we verified that TRPC5OS expression was up-regulated in breast cancer compared with adjacent normal tissues. Given the currently limited knowledge of TRPC5OS and its function in mammary tumor, we investigated its role further and showed that overexpression of TRPC5OS promoted breast cancer cell proliferation and cell cycle progression *in vitro*, and increased tumor growth in a xenograft model *in vivo*. In general, these results identified TRPC5OS as an oncogenic molecule with vital effects on breast cancer progression.

Like other microproteins, TRPC5OS may exert its functions through interactions with other proteins. Immunoprecipitation and mass spectrometry analyses showed that TRPC5OS interacted with members of the glycolytic pathway, notably ENO1. ENO1 was previously reported to be involved in the glycolytic pathway [30], and accumulating evidence has also confirmed that ENO1 is a multifunctional protein, participating in multiple biological and pathophysiological processes [29], including cell proliferation, cycle progression, invasion, and migration, indicating that it might act as an oncogene in cancer pathogenesis [30,34,38]. Feo et al. found that the ENO1 gene product could bind to the c-Myc promoter and serve as a transcriptional repressor [39]. Therefore, ENO1 mediated by TRPC5OS might be associated with Myc. However, western blotting showed that the change of Myc was not obvious after TRPC5OS overexpression. In the current study, deletion or attenuation of ENO1 inhibited mammary tumor cells proliferation, in accordance with the TRPC5OS phenotype. Furthermore, regulation of TRPC5OS levels could affect ENO1 protein levels and downstream PI3K/Akt activity as well as affecting glycolysis, as confirmed by measuring glucose uptake. Increased glucose metabolism has been shown to be important for the unlimited growth of tumor cells during the processes of tumor formation and growth [40]. The Warburg effect predicts that rapidly proliferating tumor cells will consume glucose more quickly than normal cells, even in oxygen-rich conditions [41]. This abnormal metabolic state of cancer cells was previously thought to be a side effect of alterations in signal transduction pathways caused by the deregulation of proto-oncogenes and tumor suppressors [42]. However, More and more evidence suggests that activation oncogenes and inactivation tumor suppressors could regulate cell metabolism directly, leading to tumorigenic alterations [43]. Importantly, up-regulation of ENO1 rescued the attenuation of cell proliferation caused by TRPC5OS knockdown, suggesting that ENO1 may act downstream of TRPC5OS and may be a major factor in TRPC5OS function. We therefore speculate that the phenotypes associated with TRPC5OS microprotein levels are implemented via its interaction with ENO1 protein, thus affecting metabolic homeostasis in breast cancer cells. But further researches are necessary to clarify the potential relationship between TRPC5OS and post-translational or post-transcriptome modification of ENO1. On the other hand, in a rate-limiting step for glucose metabolism, the glucose transporter

(GLUT) proteins facilitate glucose uptake across the plasma membrane [44]. Because of promoting glucose uptake, TRPC5OS might be involved in the regulation of glucose absorption by GLUT. We will verify this conjecture in the follow-up work.

Ki-67 is considered as a poor prognostic factor associated with malignant tumor characteristics such as cell proliferation, invasion, and metastasis. In the current study, we showed that patients with high levels of TRPC5OS also expressed high levels of Ki-67. TRPC5OS expression levels were also positively correlated with tumor size and tumor grade. These results therefore have potential prognostic implications. TRPC5OS may be particularly valuable in patients with triple-negative breast cancer, in whom endocrine therapies such as tamoxifen and aromatase inhibitors, as well as HER-2-targeted therapies like trastazumab and lapatinib, are ineffective due to the lack of ER, PR, and HER-2 expression.

In summary, the current study demonstrated that TRPC5OS can promote cell proliferation by interacting with ENO1. Furthermore, TRPC5OS expression levels are associated with clinicopathological features, suggesting a potential role in prognostic marker therapeutic strategies for breast cancer.

Funding

This study was supported financially by the National Natural Science Foundation of China (81672612, 81572607, 81702607, 82103007).

Data availability statement

The raw data supporting the conclusions of this article will be made available by the authors, without undue reservation. Our protein-associated data was uploaded ProteomeXchange via the PRIDE database. The associated accession number is PXD029020.

Authors' contributions

Hui Xie, Ziyi Fu, Shui Wang, Yongmei Yin and Yangyang Cui developed the experimental ideas and drafted the manuscript. Yangyang Cui, Jinghui Peng, and Mingjie Zheng conducted the experiments and contributed to the analysis of data. Han Ge, Yiqin Xia, Xiaowei Wu, and Yue Huang contributed to data analysis.

Ethics approval and consent to participate

The studies involving human participants were reviewed and approved by the Ethics Committees of the First Hospital Affiliated Hospital with Nanjing Medical University. The patients/participants provided written informed consent to participate in this study. Prior patient consent and ethics approval for the use of clinical specimens for research purposes were obtained from the Ethics Committees of the First Hospital Affiliated Hospital with Nanjing Medical University (approval number 2010-SR-091). Ethics approval for the animal studies was obtained from the Institutional Animal Care and Use Committee, Nanjing Medical University (Nanjing, China) (approval number IAUCU-1,708,006).

Credit author statement

Hui Xie, Ziyi Fu, Shui Wang, Yongmei Yin and Yangyang Cui developed the experimental ideas and drafted the manuscript.

Yangyang Cui, Jinghui Peng, and Mingjie Zheng conducted the experiments and contributed to the analysis of data.

Han Ge, Yiqin Xia, Xiaowei Wu, and Yue Huang contributed to data analysis.

Declaration of Competing Interest

We declare that there is no conflict of interests.

Acknowledgments

We thank International Science Editing (http://www.internationalscienceediting.com) for editing this manuscript.

Supplementary materials

Supplementary material associated with this article can be found, in the online version, at doi:10.1016/j.tranon.2022.101447.

References

[1] J. Ferlay, I. Soerjomataram, R. Dikshit, et al., Cancer incidence and mortality worldwide: sources, methods and major patterns in GLOBOCAN 2012, Int. J. Cancer 136 (2015) E359–E386.
[2] F. Bray, J. Ferlay, I. Soerjomataram, R.L. Siegel, L.A. Torre, A. Jemal, Global cancer statistics 2018: GLOBOCAN estimates of incidence and mortality worldwide for 36 cancers in 185 countries, CA Cancer J. Clin. 68 (2018) 394–424.
[3] X. Ma, Y. Cai, D. He, et al., Transient receptor potential channel TRPC5 is essential for P-glycoprotein induction in drug-resistant cancer cells, Proc. Natl. Acad. Sci. USA 109 (2012) 16282–16287.
[4] X. Ma, Z. Chen, D. Hua, et al., Essential role for TrpC5-containing extracellular vesicles in breast cancer with chemotherapeutic resistance, Proc. Natl. Acad. Sci. USA 111 (2014) 6389–6394.
[5] Y. Zhu, Q. Pan, H. Meng, et al., Enhancement of vascular endothelial growth factor release in long-term drug-treated breast cancer via transient receptor potential channel 5-Ca(2+)-hypoxia-inducible factor 1alpha pathway, Pharmacol. Res. 93 (2015) 36–42.
[6] P. Zhang, X. Liu, H. Li, et al., TRPC5-induced autophagy promotes drug resistance in breast carcinoma via CaMKKbeta/AMPKalpha/mTOR pathway, Sci. Rep. 7 (2017) 3158.
[7] T. Wang, K. Ning, T.X. Lu, et al., Increasing circulating exosomes-carrying TRPC5 predicts chemoresistance in metastatic breast cancer patients, Cancer Sci. 108 (2017) 448–454.
[8] H.J. Gaunt, N.S. Vasudev, D.J. Beech, Transient receptor potential canonical 4 and 5 proteins as targets in cancer therapeutics, Eur. Biophys. J. 45 (2016) 611–620.
[9] T. Ono, T. Kurashige, N. Harada, et al., Identification of proacrosin binding protein sp32 precursor as a human cancer/testis antigen, Proc. Natl. Acad. Sci. USA 98 (2001) 3282–3287.
[10] S. Ghafouri-Fard, R. Shamsi, M. Seifi-Alan, M. Javaheri, S. Tabarestani, Cancer-testis genes as candidates for immunotherapy in breast cancer, Immunotherapy 6 (2014) 165–179.
[11] W. Sun, A.Q. Li, P. Zhou, et al., DSCAM-AS1 regulates the G1 /S cell cycle transition and is an independent prognostic factor of poor survival in luminal breast cancer patients treated with endocrine therapy, Cancer Med. 7 (2018) 6137–6146.
[12] H. He, Y. Kise, A. Izadifar, et al., Cell-intrinsic requirement of Dscam1 isoform diversity for axon collateral formation, Science 344 (2014) 1182–1186.
[13] K. Sheng, J. Lu, H. Zhao, ELK1-induced upregulation of lncRNA HOXA10-AS promotes lung adenocarcinoma progression by increasing Wnt/beta-catenin signaling, Biochem. Biophys. Res. Commun. 501 (2018) 612–618.
[14] L. Shao, Z. Chen, D. Peng, et al., Methylation of the HOXA10 promoter directs miR-196b-5p-dependent cell proliferation and invasion of gastric cancer cells, Mol. Cancer Res. 16 (2018) 696–706.
[15] Q. Chu, A. Rathore, J.K. Diedrich, C.J. Donaldson, J.R. Yates 3rd, A. Saghatelian, Identification of microprotein-protein interactions via APEX tagging, Biochemistry 56 (2017) 3299–3306.
[16] D'Lima NG, J. Ma, L. Winkler, et al., A human microprotein that interacts with the mRNA decapping complex, Nat. Chem. Biol. 13 (2017) 174–180.
[17] Q. Zhang, A.A. Vashisht, J. O'Rourke, et al., The microprotein Minion controls cell fusion and muscle formation, Nat. Commun. 8 (2017) 15664.
[18] M.A. Basrai, P. Hieter, J.D. Boeke, Small open reading frames: beautiful needles in the haystack, Genome Res. 7 (1997) 768–771.
[19] S.D. Mackowiak, H. Zauber, C. Bielow, et al., Extensive identification and analysis of conserved small ORFs in animals, Genome Biol. 16 (179) (2015).
[20] D.M. Anderson, K.M. Anderson, C.L. Chang, et al., A micropeptide encoded by a putative long noncoding RNA regulates muscle performance, Cell 160 (2015) 595–606.
[21] B.R. Nelson, C.A. Makarewich, D.M. Anderson, et al., A peptide encoded by a transcript annotated as long noncoding RNA enhances SERCA activity in muscle, Science 351 (2016) 271–275.
[22] K.K. Bhati, A. Blaakmeer, E.B. Paredes, et al., Approaches to identify and characterize microProteins and their potential uses in biotechnology, Cell. Mol. Life Sci. 75 (2018) 2529–2536.
[23] Y. Hashimoto, T. Niikura, H. Tajima, et al., A rescue factor abolishing neuronal cell death by a wide spectrum of familial Alzheimer's disease genes and Abeta, Proc. Natl. Acad. Sci. USA 98 (2001) 6336–6341.

[24] C. Lee, J. Zeng, B.G. Drew, et al., The mitochondrial-derived peptide MOTS-c promotes metabolic homeostasis and reduces obesity and insulin resistance, Cell Metab. 21 (2015) 443–454.
[25] S.A. Slavoff, J. Heo, B.A. Budnik, L.A. Hanakahi, A. Saghatelian, A human short open reading frame (sORF)-encoded polypeptide that stimulates DNA end joining, J. Biol. Chem. 289 (2014) 10950–10957.
[26] W. Zhou, H. Pan, T. Xia, et al., Up-regulation of S100A16 expression promotes epithelial-mesenchymal transition via Notch1 pathway in breast cancer, J. Biomed. Sci. 21 (97) (2014).
[27] A.C. Staudt, S. Wenkel, Regulation of protein function by 'microProteins', EMBO Rep. 12 (2011) 35–42.
[28] J.P. Couso, P. Patraquim, Classification and function of small open reading frames, Nat. Rev. Mol. Cell Biol. 18 (2017) 575–589.
[29] L.E. Cabrera-Quio, S. Herberg, A. Pauli, Decoding sORF translation - from small proteins to gene regulation, RNA Biol. 13 (2016) 1051–1059.
[30] Q.F. Fu, Y. Liu, Y. Fan, et al., Alpha-enolase promotes cell glycolysis, growth, migration, and invasion in non-small cell lung cancer through FAK-mediated PI3K/AKT pathway, J. Hematol. Oncol. 8 (2015) 22.
[31] Y. Song, Q. Luo, H. Long, et al., Alpha-enolase as a potential cancer prognostic marker promotes cell growth, migration, and invasion in glioma, Mol. Cancer 13 (65) (2014).
[32] M. Zhao, W. Fang, Y. Wang, et al., Enolase-1 is a therapeutic target in endometrial carcinoma, Oncotarget 6 (2015) 15610–15627.
[33] P. Cappello, S. Rolla, R. Chiarle, et al., Vaccination with ENO1 DNA prolongs survival of genetically engineered mice with pancreatic cancer, Gastroenterology 144 (2013) 1098–1106.
[34] L. Yu, J. Shi, S. Cheng, et al., Estrogen promotes prostate cancer cell migration via paracrine release of ENO1 from stromal cells, Mol. Endocrinol. 26 (2012) 1521–1530.
[35] J. Xu, X. Huang, X. Dong, et al., Serodiagnostic Potential of Alpha-Enolase From Sarcoptes scabiei and Its Possible Role in Host-Mite Interactions, Front Microbiol. 9 (2018) 1024.
[36] P. Yonglitthipagon, C. Pairojkul, V. Bhudhisawasdi, J. Mulvenna, A. Loukas, B. Sripa, Proteomics-based identification of alpha-enolase as a potential prognostic marker in cholangiocarcinoma, Clin. Biochem. 45 (2012) 827–834.
[37] W. Zhu, H. Li, Y. Yu, et al., Enolase-1 serves as a biomarker of diagnosis and prognosis in hepatocellular carcinoma patients, Cancer Manag. Res. 10 (2018) 5735–5745.
[38] H. Qiao, Y.F. Wang, W.Z. Yuan, B.D. Zhu, L. Jiang, Q.L. Guan, Silencing of ENO1 by shRNA inhibits the proliferation of gastric cancer cells, Technol. Cancer Res. Treat. 17 (2018), 1533033818784411.
[39] S. Feo, D. Arcuri, E. Piddini, R. Passantino, A. Giallongo, ENO1 gene product binds to the c-myc promoter and acts as a transcriptional repressor: relationship with Myc promoter-binding protein 1 (MBP-1), FEBS Lett. 473 (2000) 47–52.
[40] C. Damiani, R. Colombo, D. Gaglio, et al., A metabolic core model elucidates how enhanced utilization of glucose and glutamine, with enhanced glutamine-dependent lactate production, promotes cancer cell growth: the WarburQ effect, PLoS Comput. Biol. 13 (2017), e1005758.
[41] K.O. Alfarouk, D. Verduzco, C. Rauch, et al., Glycolysis, tumor metabolism, cancer growth and dissemination. A new pH-based etiopathogenic perspective and therapeutic approach to an old cancer question, Oncoscience 1 (2014) 777–802.
[42] M.V. Liberti, J.W. Locasale, The warburg effect: how does it benefit cancer cells? Trends Biochem. Sci. 41 (2016) 211–218.
[43] R.G. Jones, C.B. Thompson, Tumor suppressors and cell metabolism: a recipe for cancer growth, Genes Dev. 23 (2009) 537–548.
[44] C.C. Barron, P.J. Bilan, T. Tsakiridis, E. Tsiani, Facilitative glucose transporters: implications for cancer detection, prognosis and treatment, Metabolism 65 (2016) 124–139.